Fluorine Substitution Effect on the Reaction Pathways of CH_3CH_2(a) and CF_3CH_2(a) on Ag(111)

W. X. Huang[†] and J. M. White*

Department of Chemistry and Biochemistry, Center for Materials Chemistry, University of Texas at Austin, Austin, Texas 78712

Received: January 26, 2004; In Final Form: March 28, 2004

The effect of fluorine substitution on the geometrical orientations and the reaction pathways of CH_3CH_2(a) and CF_3CH_2(a) on Ag(111) was investigated using temperature programmed reaction spectroscopy (TPRS) and reflection−absorption infrared spectroscopy (RAIRS). The CH_3CH_2(a) species couple to form C_4H_{10}(g) while CF_3CH_2(a) undergoes β-fluorine elimination to give $CF_2{=}CH_2$(g). On the basis of the RAIRS data, the molecular axis of CH_3CH_2(a) is oriented nearly perpendicular to the surface while that of CF_3CH_2(a) lies much nearer the surface due to the interaction between a fluorine atom and the Ag(111) surface. We propose that anchoring of CF_3CH_2(a) by both Ag−C and Ag···F interactions increases the activation energy of CF_3CH_2(a) migration compared to CH_3CH_2(a) migration and, thus, suppresses migratory coupling and facilitates β-fluorine elimination.

1. Introduction

Alkyl reactions catalyzed by transition metals are of enormous importance in many heterogeneous catalytic reactions, for example, Fischer−Tropsch synthesis, hydrocarbon conversions, and the partial oxidation of alcohols.[1−3] Many fundamental UHV studies have prepared stable alkyl groups on metal single-crystal surfaces by thermal dissociation of the C−I bond of corresponding alkyl iodides and, subsequently, have investigated the reactions of alkyl groups.[4,5] These reactions, depending on the metal substrate, include hydrogenation, complete dehydrogenation, β-hydrogen elimination to yield olefins, and alkyl coupling to yield the long-chain hydrocarbons.

Most metal surfaces preferentially dehydrogenate adsorbed alkyl groups. Only under specific conditions, such as blocking of surface sites or at high coverage of reactants, can an alkyl coupling reaction effectively compete with dehydrogenation. However, on Ag(111), alkyl groups typically selectively couple to form alkanes.[6−9] It is noteworthy that the reaction pathway of alkyls on Ag(111) can be altered by fluorine substitution in ways that depend on the fluorination position.[10−12] For example, the α-substituted species CF_3(a) is thermally stable up to 300 K on Ag(111), and above this temperature it desorbs as a radical.[10] No coupling is observed, even though the hydrogenated analogue, CH_3(a), couples at 250 K.[6] When fluorine atoms substitute for β-hydrogen, β-fluorine elimination is typical. For example, absorbed CF_3CH_2I and $CF_3CF_2CH_2I$ form $CF_2{=}CH_2$(g) and $CF_3CF{=}CH_2$(g), respectively.[11] When the adsorbed alkyls are fluorinated beyond the β-carbon position, for example, $CF_3CH_2CH_2$(a), β-dehydrogenation makes a contribution but the coupling reaction dominates.[12]

Gellman and co-workers described the fluorine substitution effect on the reaction pathways of alkyls on Ag(111) using transition state theory (TST).[12] Variable heating rate temperature programmed reaction (TPR) was employed to measure the kinetic parameters for the coupling of CH_3CH_2(a), CH_3CH_2-CH_2(a), and $CF_3CH_2CH_2$(a) on Ag(111). Their studies show that substitution of fluorine for hydrogen systematically decreases the coupling reaction rate. They proposed that the transition state for the alkyl coupling reaction on Ag(111) is electron deficient with respect to the initial state. When fluorine replaces hydrogen, the transition state is destabilized and/or the initial state is stabilized, leading to a net increase in the reaction activation barrier and hence a decrease in reaction rate.

In this paper, we approach this problem in a somewhat different way based on the following. As proposed by Zheng et al,[13] the kinetic barriers for the coupling of alkyls on metal surfaces can be decomposed as follows: preferred sites of chemisorption, differential barriers to migration on the surface, a "proximity" or crowding effect for the assembly of fragments prior to reaction, and, finally, an activation energy for actual coupling and desorption. Experimental results have shown that the coupling reactions of adsorbed alkyl groups on Ag(111) typically follow first-order kinetics rather than the second-order kinetics expected for a bimolecular recombination reaction.[6,7,14] Although there is no direct evidence on Ag, this is ascribed to islanding of alkyl groups so that the kinetics are determined by the coupling of interacting alkyls within these islands, not by the diffusion of alkyls across the surface. Supporting this model, there is strong LEED and STM evidence for islanding of methyl radicals on Cu(111).[15,16] From this perspective, fluorination could alter the reaction pathway by increasing the kinetic barrier (activation energy) for diffusion to form the islands of alkyls on the surface rather than the coupling reaction itself. While STM could, in principle, experimentally separate the kinetic parameters for diffusion from those for coupling, we take an indirect, but helpful, approach based on reflection−absorption infrared spectroscopy (RAIRS) and temperature programmed reaction spectroscopy (TPRS). The adsorption geometry differences, reflected in vibrational mode activity,[17] enable us to assess the relative migration propensity of these species. As a test of our idea, CH_3CH_2(a) and CF_3CH_2(a), created by thermally

* Corresponding author. Fax: (512) 471-9495. E-mail: jmwhite@mail.utexas.edu.

[†] Current address: Fritz-Haber-Institut der Max-Planck-Gesellschaft, D14195 Berlin, Germany.

10.1021/jp049643h CCC: $27.50
Published on Web 05/05/2004

breaking the C−I bonds of their corresponding alkyl iodides, were compared using TPRS and RAIRS.

2. Experimental Section

The experiments were conducted in a two-level stainless steel ultrahigh-vacuum (UHV) chamber.[18] The upper level is equipped with a Nicolet Magna-IR 860 spectrometer for RAIRS, a SRS RGA 200 for residual gas analysis (RGA), and an ion sputtering gun; the lower level comprises a UTI-100C mass analyzer for TPRS and a single-pass cylindrical mirror analyzer for Auger electron spectroscopy (AES). The chamber was pumped with turbomolecular pumps to a base pressure of 1.0 to 2.0 $\times$ 10^{-10} Torr.

The Ag (111) sample was mounted on a tungsten loop attached to rectangular cross section copper bars that were electrically isolated from a hollow copper block filled with liquid nitrogen. The tungsten loop was connected to a high current power supply for resistive heating of the sample. The sample temperature was controlled between 80 and 1000 K with a commercial temperature controller. A type K thermocouple inserted into a hole at the edge of the crystal was used to determine the surface temperatures.

Initially, the Ag(111) surface was cleaned by repeated cycles of Ar^+ sputtering and annealing until no contaminants could be detected by AES. Between experiments, the surface was returned to a clean state, monitored by AES, by heating to 960 K, to desorb atomic iodine and AgF.[10] The adsorbates, ethyl iodide (CH_3CH_2I, 99% purity, Aldrich) and 2,2,2-trifluoroethyl iodide (CF_3CH_2I, 99% purity, Lancaster) were used as received except for removal of dissolved gases by several cycles of freeze−pump−thaw prior to experiments. Their purities were verified by RGA.

Adsorbates were dosed through a preset leak valve ending in a capillary-array doser. The doser tube ended 2 mm in front of the sample during dosing and was retracted 25 mm after dosing. To dose, 0.38 Torr of adsorbate was added to a vessel behind a butterfly valve (closed) that was connected by an evacuated tube leading to the leak valve. The leak valve was preset so that 0.38 Torr gave a chamber pressure rise of 3.0 $\times$ 10^{-10} Torr when the temperature of all the chamber surfaces was 300 K. With the substrate cooled, the butterfly valve was opened to initiate the dose. The dose was terminated, not by closing the leak valve, but by evacuating the gas behind the leak valve with a turbomolecular pump. This procedure gave excellent experimental reproducibility (±2%) of TPD spectra. Careful calibration shows that the exposure to the surface is 30$\times$ that obtained by backfilling the chamber. Thus the reported exposures in Langmuir (1 L = 1.0 $\times$ 10^{-6} Torr•s) have been multiplied by 30, that is, exposure in L = 30 $\times$ 3 $\times$ 10^{-4} $\times$ t where t is the dose time (s). With the use of a mercury cadmium telluride (MCT) detector, RAIRS spectra were collected by coadding 1500 scans at 4 cm^{-1} resolution. RAIRS for clean Ag (111) was used as the reference. TPRS spectra were collected at a ramp rate of 1 K•s^{-1}. At most, eight different m/e values could be recorded in one experiment.

3. Results

3.1. CH_3CH_2I/Ag(111). Figure 1a presents the TPRS spectra of $C_2H_5^+$ after CH_3CH_2I doses at 90 K. Below 2 L, a single desorption peak appears at 183 K and grows with exposure. For exposures above 2.0 L, this peak broadens and there are multiple local maxima. Furthermore, new peaks arise at 99 and 128 K. The multiple $C_2H_5^+$ desorption peaks are assigned by comparing the desorption traces of $C_3H_7^+$, I^+, and $C_2H_5I^+$

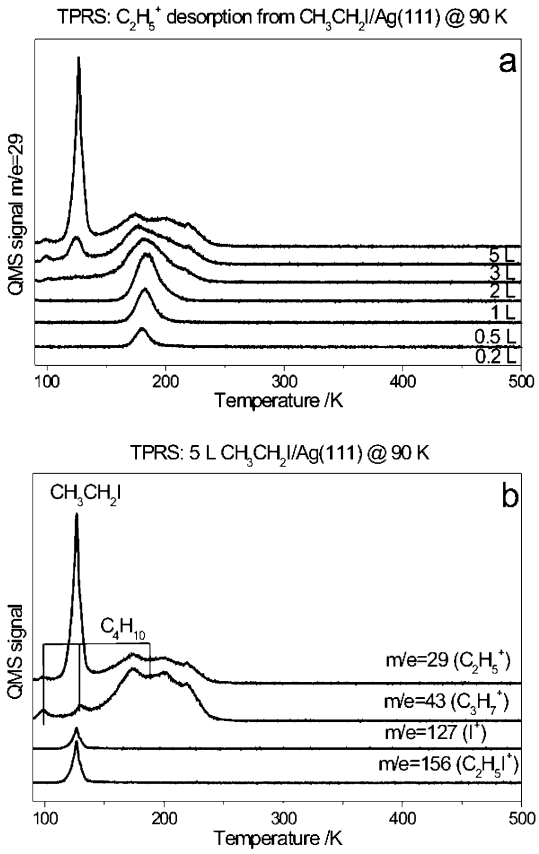

Figure 1. Temperature programmed reaction spectra following CH_3CH_2I doses on Ag(111) at 90 K.

(Figure 1b) for a 5 L CH_3CH_2I dose. The $C_2H_5^+$, I^+, and $C_2H_5I^+$ signals all peak at 128 K. Separate experiments show that this peak does not saturate with increasing dose. Thus, we assign it to desorption of multilayer C_2H_5I. The other peaks (99, 130, and 190 K) occur only for $C_2H_5^+$ and $C_3H_7^+$ and are attributed to the desorption of C_4H_{10} from the self-coupling of C_2H_5(a) (the desorption trace of C_4H_{10} is not shown). No signal attributable to monolayer C_2H_5I(a) was observed, indicating that chemisorbed CH_3CH_2I on Ag(111) prefers C−I bond rupture to desorption. The atomic iodine desorbs near 820 K (not shown). These results and assignments concur with previous reports[7] and show that CH_3CH_2(a) selectively undergoes self-coupling to form C_4H_{10} on Ag(111).

The corresponding RAIRS results for doses at 90 K are shown in Figure 2. At the lowest exposure (0.2 L), six bands centered at 1194, 1374, 1433, 2914, 2944, 2972, and 3002 cm^{-1} are observed. For doses of 0.5 and 1 L, these bands intensify and those at 2944, 2972, and 3002 cm^{-1} slightly red shift. For a dose of 2 L there are interesting changes. The intensities of bands at 1433, 2944, and 3002 cm^{-1} are much lower than are observed for a 1 L dose, and new bands appear at 1063, 1174, 1204, 2803, 2864, 2916, and 2971 cm^{-1}. For a 2 L dose, there is significant broadening of the TPRS spectrum (Figure 1) and some desorption of undissociated C_2H_5I (not shown). Increasing the dose to a 3 L exposure results in clear multilayer desorption (Figure 1) and the appearance of additional RAIRS bands at 951 and 1213 cm^{-1}. Larger exposures do not lead to any new bands; those at 951, 1174, 1204, 1213, 1377, 1443, 2864, and 2971 cm^{-1} intensify.

Previous XPS results demonstrate that monolayer CH_3CH_2I molecularly chemisorbs on Ag(111) at 90 K and dissociates into CH_3CH_2(a) and I(a) below 200 K upon heating.[7,19] Thus, molecular CH_3CH_2I(a) gives rise to the spectra of Figure 2. By

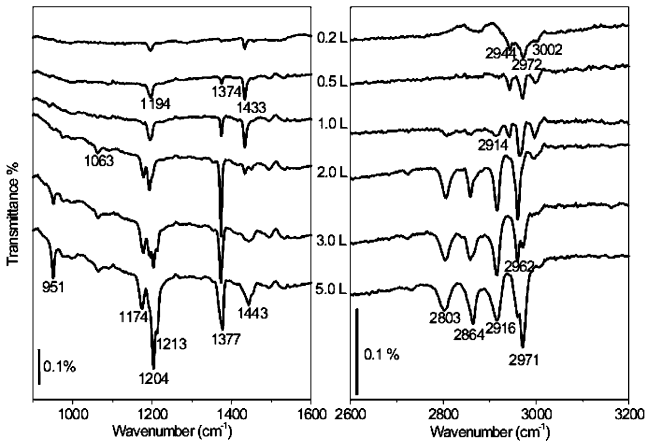

Figure 2. RAIRS spectra following CH_3CH_2I doses on Ag(111) at 90 K. All spectra were recorded at 90 K.

TABLE 1: Assignment of Observed RAIRS Bands (in cm^{-1}) for CH_3CH_2I Adsorption on Ag(111) at 90 K

assignment (symmetry)	CH_3CH_2I/Ag(111) submono-layer	mono-layer	multi-layer	CH_3CH_2I (s) (ref 17)
C−C stretch (a′)			951	949
CH_2 twist (a″)			1174	1199
CH_2 wag (a′)	1194	1194	1204	1206
C−C stretch + C−I bend			1213	1215
CH_3 sym deformation (a′)	1374	1374	1377	1370
CH_3 asym deformation (a″)	1433		1443	1433
		2803?	2803?	
2 CH_3 asym deformation (a″)		2864?	2864	2866
CH_3 sym stretch (a′)	2914	2916	2916	2908
CH_2 sym stretch (a′)	2944			2954
CH_3 asym stretch (a′)		2962		2968
CH_3 asym stretch (a″)	2972		2971	2975
CH_2 asym stretch (a″)	3002			3017

comparison with the IR spectra of solid CH_3CH_2I,[20] the observed bands are assigned to submonolayer, monolayer, and multilayer CH_3CH_2I(a) (Table 1). The 1194, 1374, and 1433 cm^{-1} modes found for low doses are assigned, respectively, to the CH_2 wag (a′ symmetry), CH_3 symmetric deformation (a′ symmetry), and CH_3 antisymmetric deformation (a″ symmetry) of submonolayer CH_3CH_2I(a). When the coverage is 1 ML (2 L dose), the CH_2 wag and CH_3 symmetric deformation modes are intense, while the CH_3 antisymmetric deformation mode is weak. For multilayers, the CH_3 antisymmetric deformation appears again at 1443 cm^{-1}. The peaks at 1174 and 1204 cm^{-1} are assigned to the CH_2 twist (a″ symmetry) and CH_2 wag, respectively, and the 951 cm^{-1} band is assigned to the C−C stretch (a′ symmetry). In multilayers, the combination band (C−C stretch + C−C−I deformation) appears at 1213 cm^{-1}. As discussed below, the RAIRS intensity variations are interpreted in terms of a coverage-dependent orientation of CH_3CH_2I(a).

3.2. CF_3CH_2I/Ag(111). The TPRS of CF_3CH_2I has been investigated in detail by Gellman and co-workers.[11] In agreement with their findings, our TPRS spectra of CF_3CH_2I on Ag(111) show the evolution of a single $C_2H_2F_2^+$ ($m/e = 64$) desorption peak around 250 K for exposures below 2 L (Figure 3a). This peak is not accompanied by peaks in the desorption traces of $C_2H_3F_2^+$ ($m/e = 83$) and I^+ ($m/e = 127$) (Figure 3b) and is attributed to the desorption of $CF_2{=}CH_2$, the β-fluorine elimination reaction product of CF_3CH_2(a). Doses exceeding 2 L result in three additional $C_2H_2F_2^+$ desorption peaks accompanied by peaks in the $CF_3CH_2^+$ and I^+ profiles. The 113 K peak is assigned to multilayer desorption. The intensity ratio, $C_2H_2F_2^+$ to $CF_3CH_2^+$, (Figure 3b) is greater at 153 than 175 K, indicating

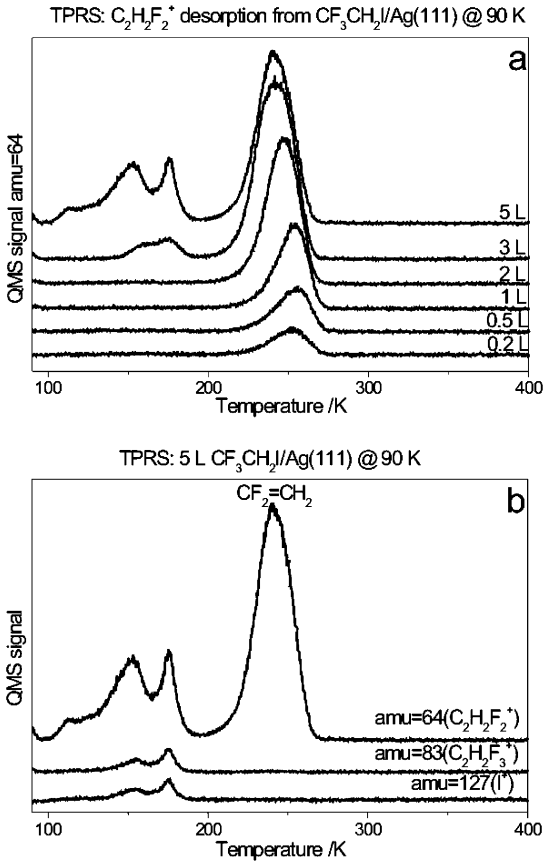

Figure 3. Temperature programmed reaction spectra following CF_3CH_2I doses on Ag(111) at 90 K.

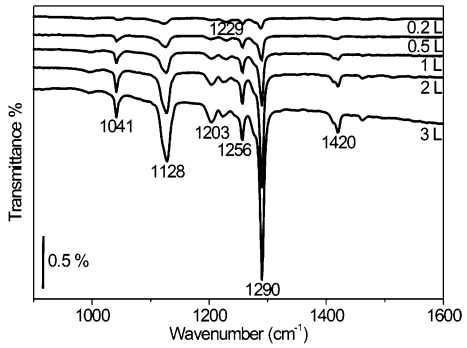

Figure 4. RAIRS spectra following CF_3CH_2I doses on Ag(111) at 90 K. All spectra were recorded at 90 K.

that at least two species are involved. While not clearly identified, other work suggested products induced by the stray electrons from the ionizer region of the mass spectrometer.[11] We propose that one peak may come from monolayer chemisorbed CF_3CH_2I(a). The results of Figure 3 reproduce earlier work and confirm that CF_3CH_2(a) selectively undergoes β-fluorine elimination.[11]

The RAIRS spectra of CF_3CH_2I are simpler than those of CH_3CH_2I (Figure 4). A 0.2 L dose of CF_3CH_2I gives rise to vibrational peaks at 1044, 1122, 1204, 1229, 1258, 1288, and 1416 cm^{-1}. These are attributed to CF_3CH_2I(a) on Ag(111). Increased dosing intensifies all the bands except that at 1229 cm^{-1}. There is also a very weak vibrational band at 2930 cm^{-1} assigned to C−H stretching (not shown). By comparing the IR of liquid CF_3CH_2I,[20] the following assignments are made (Table 2). The band at 1229 cm^{-1} is assigned to the CH_2 wag of CF_3CH_2(a). The appearance of CF_3CH_2(a) implies that some C−I rupture of CF_3CH_2I occurs at 90 K on Ag(111) (likely on

TABLE 2: Assignment of Observed RAIRS Bands (in cm^{-1}) for CF_3CH_2I Adsorption on Ag(111) at 90 K

assignment (symmetry)	CF_3CH_2I (a)/ Ag(111)	CF_3CH_2I (l) (ref 18)
C−F sym stretch (a′)	1041	1049
C−F sym stretch (a′)	1128	1114
CH_2 wag (a′)	1203	1211
CH_2 deformation (a′)	1256	1257
CH_2 twist (a″)	1290	1288
C−F asym stretch (a″)	1420	1423

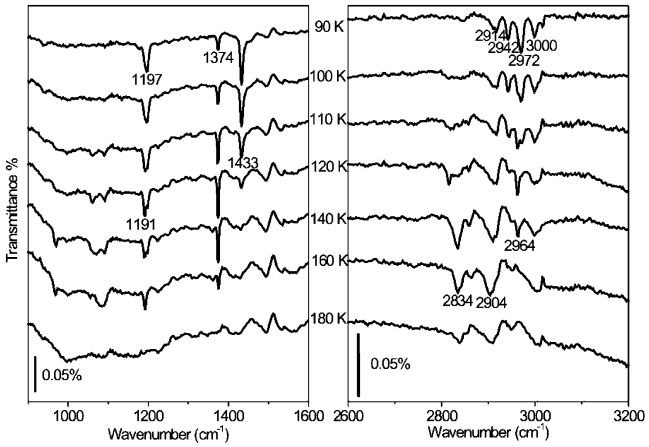

Figure 5. RAIRS spectra of 0.5 L CH_3CH_2I doses on Ag(111) at 90 K followed by annealing at the indicated temperatures for 2 min. All spectra were recorded at 90 K.

defect sites). In agreement with previous findings,[19] this result indicates that the substitution of the β-H of CH_3CH_2I by fluorine facilitates the C−I bond rupture on Ag(111).

3.3. CH_3CH_2(a)/Ag(111) and CF_3CH_2(a)/Ag(111). The above TPRS results confirm that fluorine substitution on the β-carbon renders coupling negligible in favor of β-defluorination. The thermal behavior of submonolayers of CH_3CH_2(a) and CF_3CH_2(a) monitored by RAIRS after stepwise annealing provides useful insight.

The RAIRS spectra following a dose of 0.5 L CH_3CH_2I change significantly upon annealing in steps from 90 to 180 K (Figure 5). As the annealing temperature increases (1) the 1433 cm^{-1} (CH_3 antisymmetric deformation, a″ symmetry) mode attenuates and disappears at 140 K, (2) the 1374 cm^{-1} (CH_3 symmetric deformation, a′ symmetry) mode increases up to 120 K before decreasing, (3) the 1197 cm^{-1} (CH_2 wag, a′ symmetry) mode begins to attenuate after annealing at 120 K, (4) the 1191 cm^{-1} mode appears after annealing at 110 K, grows with increasing temperature to 160 K, and vanishes after annealing at 180 K, (5) in the C−H stretching region, bands at 2904 cm^{-1} (CH_3 symmetric stretch, a′) and 2964 cm^{-1} (CH_3 antisymmetric stretch, a′) grow between 90 and 120 K at the expense of the bands at 2942 cm^{-1} (CH_2 symmetric stretch, a′) and 2972 cm^{-1} (CH_3 antisymmetric stretch, a″ symmetry), and (6) above 120 K, the peak at 2964 cm^{-1} loses intensity and disappears after 160 K and is replaced by a new peak at 2834 cm^{-1} that emerges between 120 and 160 K and vanishes at 180 K.

On basis of intensity changes, the bands can be divided into two groups. The first group includes the bands at 1191, 2834, and 2904 cm^{-1}, that appear at 120 K, grow to 160 K, and vanish at 180 K. Consistent with TPRS, this group is attributed to CH_3CH_2(a) formed by C−I rupture with assignments, as indicated in Table 3, to the CH_2 wag, CH_2 stretch, and CH_3 stretch of CH_3CH_2(a). The large red shift (108 cm^{-1}) of the CH_2 stretch in passing from CH_3CH_2I(a) to CH_3CH_2(a) is attributed to C−H mode-softening in CH_3CH_2(a). Similar mode-softening has been reported for alkyl groups bound to Cu(111).[22] The disappearance of RAIRS intensity after 180 K annealing is consistent with self-coupling to form and desorb C_4H_{10}.

TABLE 3: Assignment of Observed RAIRS Bands (in cm^{-1}) for CH_3CH_2(a) and CF_3CH_2(a) on Ag(111) at 90 K

assignment	CH_3CH_2(a)	assignment	CF_3CH_2(a)
CH_2 wag	1191	C−F stretch	1012
CH_2 stretch	2834	C−F stretch	1117
CH_3 stretch	2904	CH_2 deformation	1229
		C−F stretch	1411

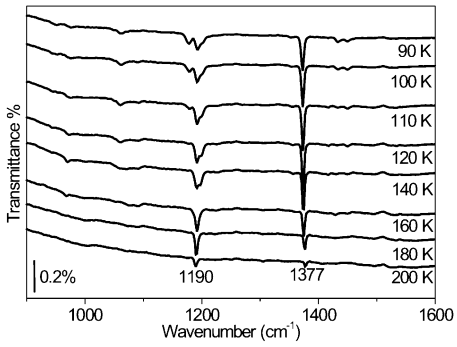

Figure 6. RAIRS spectra of 2 L CH_3CH_2I doses on Ag(111) at 90 K followed by annealing at the indicated temperatures for 2 min. All spectra were recorded at 90 K.

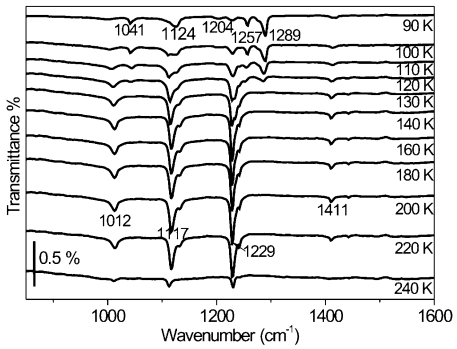

Figure 7. RAIRS spectra of 0.5 L CF_3CH_2I doses on Ag(111) at 90 K followed by annealing at the indicated temperatures for 2 min. All spectra were recorded at 90 K.

The second group comprises the 1197, 1374, 2904, and 2964 cm^{-1} bands that grow between 90 and 120 K and the 1433, 2942, and 2972 cm^{-1} bands that decay. Reorientation of submonolayer CH_3CH_2I(a) on Ag(111) upon heating accounts for these changes, and assignments are given in Table 1. These bands all attenuate at 120 K as C−I bonds break while those at 1191 and 2834 cm^{-1} grow reflecting the formation of CH_3CH_2(a).

Unlike lower doses, annealing to 200 K a 1 ML (2 L) dose of CH_3CH_2I does not lead to changes that point to adsorbate reorientation (Figure 6). While annealing above 140 K leads to changes, that is, the band at 1394 cm^{-1} weakens while that at 1191 cm^{-1} intensifies, these clearly belong to different species.

Turning to the fluorinated counterpart, annealing a 0.5 L dose of CF_3CH_2I leads to interesting contrasts between the RAIRS behavior of CF_3CH_2(a) and CH_3CH_2(a) (Figure 7). The bands at 1041, 1124, 1204, 1257, and 1289 cm^{-1}, assigned to CF_3CH_2I(a), attenuate with increasing temperature and completely disappear after 120 K annealing. Meanwhile, the bands at 1012, 1117, 1229, and 1411 cm^{-1} grow to 120 K and remain constant to 220 K. These four bands belong to CF_3CH_2(a), and we assign them to the CF stretch, another CF stretch, CH_2 deformation, and a third CF stretch, respectively (Table 3). The spectra indicate that submonolayer CF_3CH_2I(a) completely

TABLE 4: Angle (θ) between the C−C Bond and the Surface for CH_3CH_2I(a) on Ag(111) at Various Coverages and Temperatures

CH_3CH_2I dosing at 90 K		θ	0.5 L CH_3CH_2I(a)/ Ag(111)	θ
	0.2 L	29°	$T = 90$ K	22°
<1 ML	0.5 L	24°	$T = 100$ K	28°
	1 L	31°	$T = 110$ K	40°
1 ML		90°	$T = 120$ K	64°
	2 L	73°	$T = 140$ K	90°
>1 ML	3 L	65°		
	5 L	60°		

dissociates into CF_3CH_2(a) after annealing at 120 K, providing additional evidence that the substitution of β-H of CH_3CH_2I by fluorine facilitates the C−I bond rupture. The intensities all decay upon heating to 240 K, consistent with the β-F rearrangement to form and desorb $CF_2{=}CH_2$.

4. Discussion

4.1. Coverage- and Temperature-Dependent Orientation of CH_3CH_2I(a) on Ag(111). The orientation of adsorbed molecules can be deduced through symmetry analysis of observed RAIRS bands on the basis of the surface infrared spectroscopy selection rule.[16] As for alkyl halides on Pt(111),[23,24] our results imply a coverage-dependent orientation of CH_3CH_2I(a) on Ag(111) at 90 K (Figure 2).

The appearance of both the CH_3 symmetric deformation and CH_3 asymmetric deformation for coverages of CH_3CH_2I(a) at 90 K that are well below a monolayer argues for a C−C bond that is neither perpendicular nor parallel to the Ag(111) surface. The chemisorbed geometry suddenly changes as the coverage reaches 1 ML. The CH_3 asymmetric deformation becomes very weak, and the CH_3 symmetric deformation becomes very strong, both indicating that the C−C bond of 1 ML CH_3CH_2I(a) is perpendicular to the surface. Parenthetically, the absence of a C−C stretching mode may be explained by its low cross section.[23] The CH_3 asymmetric deformation reappears again for multilayers, implying that the ensemble average multilayer CH_3CH_2I(a) has a C−C bond lying in a plane that lies between the surface plane and a plane perpendicular to the surface. The CH_2 scissors mode is absent at all coverages while the CH_2 wag is clearly visible, implying that the methylene H−C−H plane is close to parallel to the surface.

From the above discussion, the main difference among the orientations for submonolayer, monolayer, and multilayer CH_3CH_2I(a) lies in the C−C bond orientation. Fan and Trenary proposed that the orientation of the C_3 axis of CH_3 groups on metal surfaces (for example, the C−C axis of ethylidyne/Pt (111)) could be roughly estimated using[24]

$$\tan^2\theta = \frac{\nu_s A_{as}}{\nu_{as} A_s} \qquad (1)$$

where θ is the angle between the C−C axis and the surface normal, ν_s and A_s are the wavenumber and intensity of the symmetric vibrational mode of the CH_3 group, and ν_{as} and A_{as} are the wavenumber and intensity of the corresponding asymmetrical vibrational mode. Using the observed CH_3 symmetric deformation (1374 cm^{-1}) and CH_3 asymmetric deformation (1433 cm^{-1}) bands, we calculated the angle between the C−C bond of CH_3CH_2I(a) and the Ag(111) surface for various coverages at 90 K (Table 4).

The orientation of submonolayer CH_3CH_2I(a) is also temperature-dependent. Between 90 and 120 K, the CH_3 asymmetric deformation mode of CH_3CH_2I(a) attenuates to negligible intensity, while the CH_3 symmetric deformation mode intensifies (Figure 5). This is consistent with movement with increasing temperature from a tilted toward a perpendicular orientation as the temperature increases (Table 4). It is noteworthy that, on the basis of the observed RAIRS bands, submonolayer CH_3CH_2I(a) at 120 K is oriented as monolayer CH_3CH_2I(a) at 90 K. However, since the C−I stretching mode lies outside the detectable range of RAIRS, we have no direct information of the orientation of the C−I bond, that is, the orientation of the molecular plane. For multilayer CH_3CH_2I(a) at 90 K, the observation of the combination band (C−C stretch + C−C−I deformation) suggests that the molecular plane is perpendicular to the surface. This combination band is absent for submonolayer CH_3CH_2I(a) at 120 K. With this constraint, we propose that submonolayer CH_3CH_2I(a) takes the following orientation on Ag(111) at 120 K: the C−I bond lies parallel to the surface and the C−C bond is perpendicular with the surface. Such an orientation is reasonable for a precursor to undergo C−I bond breaking.

4.2. Orientation of CF_3CH_2I(a) on Ag(111). The orientation of CF_3CH_2I(a) does not exhibit a coverage or temperature dependence. The relatively strong symmetric and asymmetric C−F stretch modes indicate that the C−C bond is tilted with respect to the surface normal and the surface plane. Meanwhile, the presence of the CH_2 wag and CH_2 scissors modes implies, unlike the case for CH_3CH_2(a), that the CH_2 plane is also tilted away from the surface.

4.3. Fluorination Effect on the C−I Rupture Reaction on Ag(111). The RAIRS results clearly show that the C−I bond is more readily broken for CF_3CH_2I(a) than for CH_3CH_2I(a) on Ag(111). The C−I rupture of CF_3CH_2I(a) begins at 90 K and is completed below 140 K while, for CH_3CH_2I(a), cleavage occurs between 120 and 160 K. This indicates that the fluorination reduces the activation energy for the C−I rupture reaction, which is consistent with earlier work that shows that the reduction of the activation barrier is attributed to both the field and the polarizibility effects of the CF_3 group.[19]

4.4. Fluorination Effect on the Orientation of Alkyl groups on Ag(111). RAIRS results indicate that CH_3CH_2(a) and CF_3CH_2(a) take quite different orientations on Ag(111). The CH_3CH_2(a) gives only three RAIRS bands that, in the corresponding CH_3CH_2I molecule, possess a′ symmetry. This suggests a C−C bond axis oriented perpendicular to the Ag(111) surface. The observation of the CH_3 stretch mode at 2904 cm^{-1} (CH_3 symmetric stretch in CH_3CH_2I), not that at 2972 cm^{-1} (CH_3 asymmetric stretch in CH_3CH_2I), is also consistent with this orientation. The absence of a C−C stretching mode, again, is attributed to its low cross section.[23]

The case is different for CF_3CH_2(a) on Ag(111). Bands that have both a′ and a″ symmetry in CF_3CH_2I are clearly visible. The appearance of C−F stretch modes at 1012/1117 and 1411 cm^{-1}, corresponding to the symmetric and asymmetric stretch vibrations in CF_3CH_2I, implies a C−C bond axis tilted with respect to the surface normal and the surface plane. We attribute the tilted orientation of the C−C bond to the strong interaction between at least one fluorine atom and the Ag substrate ($E_{Ag-F} \sim 85$ kcal/mol[25]); thus, CF_3CH_2(a) is anchored by both the Ag−C bond and the Ag···F interaction.

4.5. Relationship between the Molecular Orientation and Reaction Pathway of Alkyl Groups on Ag(111). TPRS results show that fluorination completely changes the reaction pathway from self-coupling for CH_3CH_2(a) to β-fluorine elimination for CF_3CH_2(a). The enthalpy change (ΔH) of alkyl reactions on

Ag(111) has been estimated to be −48 kcal/mol for coupling and −5 kcal/mol for fluorine elimination, respectively.[11] Since the self-coupling reaction is thermodynamically favored, the change of reaction pathway is attributed to a kinetic effect, that is, fluorination of the β-position increases an activation barrier in some step leading to the coupling product enough to make β-fluorine elimination favored.

Previous TPRS studies have established that alkyl coupling on Ag(111) follows first-order kinetics.[6,7,14] This has been discussed in terms of alkyl groups diffusing rapidly to form islands on Ag(111) from which nearest neighbor pairs link in a rate-determining unimolecular process. Organized islands of methyl radicals on Cu(111) have recently been imaged.[15,16] These results clearly demonstrate that the formation of islands via the migration of alkyl fragments is determinative of the kinetics of coupling reactions on copper. Thus, when considering the fluorination effect on the kinetics of the alkyl coupling reaction, one must consider two aspects: both the effect on the activation barrier of the reaction itself and that on the activation barrier of the migration of alkyl groups to form islands on the surface. We propose that, compared to CH_3CH_2(a), fluorination of the β-position as in CF_3CH_2(a) increases the activation barrier of surface diffusion to an extent that island formation and, thus, the self-coupling reaction can no longer compete with the β-fluorine elimination reaction. The different geometries of CH_3CH_2(a) and CF_3CH_2(a) on Ag(111) are consistent with this proposal. CH_3CH_2(a) is likely much more mobile than tilted CF_3CH_2(a) that is anchored by both the Ag−C bond and Ag···F interaction.

Gellman and co-workers have systemically measured the activation energy of the coupling reaction for alkyls and fluorinated-alkyls (beyond the β-position) on Ag(111) and found that fluorination increases the activation energy of the coupling reaction.[12] On basis of these results, they proposed that the transition state for the alkyl coupling reaction on Ag(111) is electron deficient with respect to the initial state. When hydrogen is substituted by fluorine, the transition state is destabilized and/or the initial state is stabilized, leading to a net increase in the reaction activation barrier. If alkyl diffusion controls alkyl coupling on Ag(111), then the activation barrier for alkyl migration on the surface may be the critical elementary step. If so, the findings of Gellman and co-workers would be interpreted in terms of fluorination increasing the activation energy of the diffusion process.

Our proposal can also explain the effect of the fluorination position on the reaction pathway of alkyl groups on Ag(111). It is reasonable that the Ag···F interaction decreases with the increasing Ag−F distance. Thus, $CF_3CH_2CH_2$(a) could be more mobile than CF_3CH_2(a) and CF_3(a) on Ag(111). This is consistent with observations: the coupling reaction is the major reaction pathway for $CF_3CH_2CH_2$(a) on Ag(111) but is completely blocked for CF_3CH_2(a) and CF_3(a) on Ag(111).

It is worthwhile mentioning that the reaction pathways of CH_3(a) on Cu(111) and Au(100) were observed to change when surface iodine and $P(CH_3)_3$ coexisted on the surfaces.[26,27] Coexisting with high coverages of I(a) or $P(CH_3)_3$(a), CH_3(a) desorbs as radicals instead of coupling to produce higher hydrocarbons. The effect of coadsorbates is to inhibit the competing reactions of CH_3(a), not to alter the metal−CH_3 bond. Obviously, one possibility is that the coadsorbates increase the barrier for CH_3(a) migration, thereby inhibiting the coupling reaction and, thus, favoring desorption as radicals.

5. Conclusion

We have employed RAIRS and TPRS to investigate the effects of fluorination on the orientation and subsequent reaction pathway of alkyl groups on Ag(111). The orientation of adsorbed ethyl iodide (CH_3CH_2I(a)) is coverage- and temperature-dependent. The corresponding CF_3CH_2I(a) orientation does not vary significantly.

Upon C−I dissociation, adsorbed alkyl fragments are formed. With an upright orientation, ethyl group (CH_3CH_2(a)) undergoes migratory self-coupling reaction to give gaseous C_4H_{10} on Ag(111). Fluorination at the β-position changes the reaction pathway. Due to the Ag···F interaction, CF_3CH_2(a) takes a tilted orientation and selectively undergoes a β-fluorine elimination reaction. We attribute the reaction pathway change to the anchoring of CF_3CH_2(a) on the surface by both the Ag−C bond and Ag···F interaction, which increases the barrier to migration of CF_3CH_2(a) to form islands essential for the following coupling reaction and thus blocks the migratory self-coupling reaction.

Acknowledgment. The work is supported by the Chemical Sciences, Geosciences and Biosciences Division, Office of Basic Energy Services, Office of Science, U.S. Department of Energy, and by the Robert A. Welch Foundation.

References and Notes

(1) Anderson, R. B. *The Fischer−Tropsch Synthesis*; Academic Press: New York, 1984.
(2) Barteau, M. A.; Madix, R. A. In *The Chemical Physics of Solid Surfaces and Heterogeneous Catalysis*; King, D. A., Woodruff, D. P., Eds.; Elsevier: Amsterdam, 1982; Vol. 4.
(3) Kemball, C. *Catal. Rev. Sci. Eng.* **1971**, *5*, 33.
(4) Zaera, F. *Chem. Rev.* **1995**, *95*, 2651.
(5) Bent, B. E. *Chem. Rev.* **1996**, *96*, 1361.
(6) Zhou, X. L.; Solymosi, F.; Blass, P. M.; Cannon, K. C.; White, J. M. *Surf. Sci.* **1989**, *219*, 294.
(7) Zhou, X. L.; White, J. M. *Catal. Lett.* **1989**, *2*, 375.
(8) Zhou, X. L.; White, J. M. *J. Phys. Chem.* **1991**, *95*, 5575.
(9) Zhou, X. L.; Blass, P. M.; Koel, B. E.; White, J. M. *Surf. Sci.* **1992**, *271*, 427.
(10) Castro, M. E.; Pressley, L. A.; Kiss, J.; Pylant, E. D.; Jo, S. K.; Zhou, X. L.; White, J. M. *J. Phys. Chem.* **1993**, *97*, 8476.
(11) Paul, A.; Gellman, A. J. *Langmuir* **1995**, *11*, 4433.
(12) Paul, A.; Gellman, A. J. *J. Am. Chem. Soc.* **1995**, *117*, 9056.
(13) Zheng, C.; Apeloig, Y.; Hoffmann, R. *J. Am. Chem. Soc.* **1988**, *110*, 749.
(14) Wu, H. J.; Hsu, H. K.; Chiang, C. M. *J. Am. Chem. Soc.* **1999**, *121*, 4433.
(15) Chuang, P.; Chan, Z. L.; Chien, S. H.; Song, K. J.; Klauser, R.; Chuang, T. J. *Langmuir* **2002**, *18*, 4549.
(16) Chan, Y. L.; Pai, W. W.; Chuang, T. J. *J. Phys. Chem. B* **2004**, *108*, 815.
(17) Chabal, Y. J. *Surf. Sci. Rep.* **1988**, *8*, 214.
(18) Huang, W. X.; White, J. M. *Surf. Sci.* **2002**, *513*, 399.
(19) Buelow, M. T.; Gellman, A. J. *J. Am. Chem. Soc.* **2001**, *123*, 1440.
(20) Durig, J. R.; Thompson, J. W.; Thyagesan, V. W.; Witt, J. D. *J. Mol. Struct.* **1975**, *24*, 41.
(21) Harnish, D. F.; Hirschmann, R. P. *Appl. Spectrosc.* **1970**, *24*, 28.
(22) Lin, J. L.; Bent, B. E. *Chem. Phys. Lett.* **1992**, *194*, 208.
(23) Zaera, F.; Hoffmann, H.; Griffiths, P. R. *J. Electron. Spectrosc. Relat. Phenom.* **1990**, *54/55*, 705.
(24) Fan, J. F.; Trenary, M. *Langmuir* **1994**, *10*, 3649.
(25) *CRC Handbook of Chemistry and Physics*, 70th ed.; CRC Press: Boca Raton, FL, 1989−1990.
(26) Lin, J. L.; Bent, B. E. *J. Am. Chem. Soc.* **1993**, *115*, 2849; *J. Phys. Chem.* **1993**, *97*, 9713.
(27) Paul, A.; Bent, B. E. *J. Catal.* **1994**, *147*, 264.